TABLE II

RATE CONSTANTS FOR CHLORIDE LOSS FROM Pt(Me$_2$en)Cl$_2$ in 1:1 ETHANOL–H$_2$O AT 25°

[Acetate], M	pH	k_{obsd}, sec^{-1}
0	5.5	1.11×10^{-5}
0	$[OH^-] = 0.05\ M$	1.00×10^{-5}
0.04	6.5	1.02×10^{-5}
1.00	6.76	1.03×10^{-5}

reaction mixtures at the end of the reaction with silver nitrate revealed that both chloride ions had been liberated. The product was the same in all four reactions, presumably the hydrolysis product.

Even with a poor ligand such as carboxylate ion the neighboring group effect is displayed. Although free acetate ion does not react with a similar complex, when chelation is possible then the incoming carboxylate ion assists the elimination of the coordinated chloride ion. The amount of assistance determines whether the monochloro or diacetato complex is formed. The increased rate of reaction of the carboxylate ion over the carboxylic acid group is due to the entropy term rather than a lowering of the activation energy. The activation energies for the substitution of the first chloride ion are the same in both cases. The larger entropy of activation for the carboxylate ion reaction is consistent with an internal S$_N$2 displacement of the chloride ion. The activation energy for replacement of the second chloride ion is higher by about 5 kcal. This could explain the lack of reaction of the carboxylic acid group, since the entropy of activation would be expected to be much lower than for the reaction of the conjugate base. Also the ring-opening reaction would be expected to be acid catalyzed, and this would help to push the equilibrium completely over toward the monochloro complex.

The fact that the activation energy for the formation of the second chelate ring to give the diacetatoplatinum(II) complex is higher than that for the formation of the first ring seems to indicate that some steric strain is involved.

The pronounced dependence of the reaction of Pt(H$_2$EDDA)Cl$_2$ on pH can be contrasted with the reaction of the quinquedentate [Co(HEDTA)Cl]$^-$ to give Co(EDTA). The rate of the latter reaction is virtually independent of pH.[6,7] It was suggested that the carboxylate ion group could not assist the elimination of a negatively charged ligand due to electrostatic repulsion. The present work shows that the same reasoning cannot be applied to the complexes of platinum(II). The S$_N$2 character of the reaction of platinum(II) complexes leads to marked anchimeric assistance effects, whereas the S$_N$1 character of the cobalt(III) reactions does not allow such assistance.

Acknowledgment.—This work was supported by the U. S. Atomic Energy Commission under Contract At(11-1)-1087.

---

(6) R. Dyke and W. C. E. Higginson, *J. Chem. Soc.*, 1998 (1960).

(7) M. L. Morris and D. H. Busch, *J. Phys. Chem.*, **63**, 340 (1959).

CONTRIBUTION FROM THE W. A. NOYES LABORATORY,
UNIVERSITY OF ILLINOIS, URBANA, ILLINOIS

Crystal Field Analysis of the Spectra of Tetragonal Nickel(II) Pyridine Complexes

BY DAVID A. ROWLEY[1] AND RUSSELL S. DRAGO

Received December 15, 1966

The optical absorption spectra of mulls of Ni(py)$_4$Br$_2$ and Ni(py)$_4$Cl$_2$ have been determined at liquid nitrogen temperature The splitting of the absorption bands due to the strong axial field is discussed using crystal field theory. Assignments are made and agreements between experiment and theory are excellent. The difference between solution and solid data is discussed. The Dq's of Cl$^-$ and Br$^-$ were calculated to be 680 and 600 cm^{-1}, respectively.

Introduction

In the course of investigating[2,3] some pyridine complexes of nickel(II), we noticed some interesting properties in the electronic absorption spectrum of the tetragonal complexes. There has been a great deal of interest in tetragonal metal complexes[4–8] with much of the work being centered on Co(III) and little attention being paid to Ni(II). The appearance of "extra" bands in Ni(py)$_4$Cl$_2$ was taken as evidence for tetragonal distortion,[9] but a complete interpretation of the spectra was not attempted.

The complexes chosen for this study are Ni(py)$_4$X$_2$ where X$^-$ = Cl$^-$ and Br$^-$. These have been shown to be paramagnetic with the X groups occupying the *trans* positions.[10,11] Both of these complexes are ideally suited for analysis because the electronic spectrum

---

(1) Abstracted in part from the Ph.D. thesis of D. A. Rowley, University of Illinois, Urbana, Ill.

(2) M. R. Rosenthal and R. S. Drago, *Inorg. Chem.*, **4**, 840 (1965).

(3) M. R. Rosenthal and R. S. Drago, *ibid.*, **5**, 492 (1966).

(4) R. A. D. Wentworth and T. S. Piper, *ibid.*, **4**, 709 (1965).

(5) R. A. D. Wentworth and T. S. Piper, *ibid.*, **4**, 1524 (1965).

(6) D. M. L. Goodgame, *et al.*, *ibid.*, **5**, 635 (1966).

(7) R. A. D. Wentworth, *ibid.*, **5**, 496 (1966).

(8) W. A. Baker, Jr., and M. S. Phillips, *ibid.*, **5**, 1042 (1966).

(9) O. Böstrup and C. K. Jørgensen, *Acta Chem. Scand.*, **11**, 1223 (1957).

(10) M. A. Porai-Koshits, *Tr. Inst. Kristallogr. Akad. Nauk SSSR*, **10**, 117 (1954).

(11) A. S. Antsishkina and M. A. Porai-Koshits, *Kristallografiya*, **3**, 676 (1958).

contains bands in excess of those needed to fit the parameters which can then be used to check the model.

We have chosen to interpret our results in terms of crystal field theory. The crystal field theory for tetragonal d^8 metal complexes has been developed by Maki from a weak-field point of view[12] and from a strong-field point of view by Hare and Ballhausen.[13] Fenske, *et al.*, have developed the complete theory, including spin–orbit coupling, for tetragonal d^8 systems.[14] Here we have extended the theory of Hare and Ballhausen to include the singlet states using methods outlined by Ballhausen.[15]

Theory and Calculations

The determination of the transition energies requires a solution to the Schroedinger equation: $\mathcal{H}\Psi = E\Psi$ where

$$\mathcal{H} = \sum_i -(\hbar^2/2m)\nabla_i^2 - (Ze^2/r_i) + \sum_{i>j}(e^2/r_{ij}) + \sum_i V^{\mathrm{CF}}(r_i) \qquad (1)$$

All terms have the usual significances, and $V^{\mathrm{CF}}(r_i)$ is the crystal field operator for a molecule with D_{4h}[16] symmetry. Spin–orbit coupling has been omitted.

Since we are interested in differences for transition energies, the first two terms of eq 1 need not be evaluated as these are assumed to be constant. Evaluation of the matrices whose elements are given by

$$H_{nm} = \langle\Psi_n|\mathcal{H}'|\Psi_m\rangle$$

where

$$\mathcal{H}' = \sum_{i>j}(e^2/r_{ij}) + \sum_i V^{\mathrm{CF}}(r_i)$$

yields the matrix equation

$$\mathbf{E} = \mathbf{B} + \mathbf{C} + \mathbf{Dq} + \mathbf{Ds} + \mathbf{Dt}$$

or

$$\mathbf{E} = B\mathbf{M} + C\mathbf{M}' + Dq\mathbf{M}'' + Ds\mathbf{M}''' + Dt\mathbf{M}''''$$

where B and C are the Racah parameters and Dq, Ds, and Dt represent the parameters associated with V^{CF}.[17] The H_{nm} values for the singlet states were determined by use of strong-field wave functions using the techniques described by Hare and Ballhausen.[10,15] The results are presented in Table I.

The observed spectra are fitted to the theory by varying the parameters Dq, Ds, Dt, B, and C. The parameter C arises only in the spin-forbidden transitions. This was done by solving the matrix equation with the use of a program developed at this laboratory by Mr. D. H. Dugre. This program is a minimum-seeking routine which varies the coefficients of the energy matrices, B, Dq, Ds, and Dt, until the best fit of experimental data is obtained or until the calculated energies agree with the observed energies within experimental error. A least-squares error sum is used as the criterion of the best fit. Then C is obtained by fitting the low-energy spin-forbidden band.

TABLE I

MATRIX ELEMENTS FOR SINGLET STATES

State				
Free ion	O_h	D_{4h}	*Ds*	*Dt*
^1D	^1E_g	$^1B_{1g}$	$+2$	-8
		$^1A_{1g}$	-2	$-^4/_3$
^1G	^1E_g	$^1B_{1g}$	0	7
		$^1A_{1g}$	0	7
^1S	$^1A_{1g}$	$^1A_{1g}$	0	$-^{14}/_3$
^1G	$^1A_{1g}$	$^1A_{1g}$	0	7
^1G	$^1T_{2g}$	$^1B_{2g}$	2	-8
		$^1E^a{}_g$	-1	-3
^1D	$^1T_{2g}$	$^1B_{2g}$	0	7
		$^1E^b{}_g$	0	$-^7/_4$
^1G	$^1T_{1g}$	$^1A_{2g}$	-4	2
		$^1E^c{}_g$	2	$^3/_4$
	$\langle ^1E^b{}_g\|V_{\mathrm{CF}}\|^1E^c{}_g\rangle$		$\sqrt{3}$	$^5/_4\sqrt{3}$

Since the relationship between the crystal field parameters and those of the molecular orbital approach, as described by McClure,[18] will be of use later, these are given below

$$\delta\pi = \frac{-3Ds + 5Dt}{2} \qquad (2)$$

$$\delta\sigma = \frac{-12Ds - 15Dt}{8} \qquad (3)$$

Experimental Section

Preparation of Complexes.—All chemicals used were of reagent grade quality and used without further purification.

The complexes were prepared by the following general procedure. The aquated metal halides were dissolved in a minimum amount of absolute ethanol, then dehydrated with 2,2-dimethoxypropane by stirring with a magnetic stirrer for 2 hr at room temperature. The resulting solutions were treated with a large excess of pyridine and the complex immediately precipitated. The resultant slurry was then stirred for an additional 1 hr. The complexes were then collected and washed with ether. These were then dried under vacuum for 0.5 hr at room temperature.

Anal. Calcd for $Ni(C_5H_5N)_4Cl_2$: C, 53.95; N, 12.59; H, 4.53; Ni, 13.20. Found: C, 53.37; N, 12.03; H, 4.57; Ni, 12.77. Calcd for $Ni(C_5H_5N)_4Br_2$: C, 44.96; N, 10.50; H, 3.78; Ni, 11.00. Found: C, 44.70; N, 10.01; H, 3.64; Ni, 10.76.

Spectrophotometric Measurements.—Near-infrared and visible absorption spectra were obtained using a Cary spectrophotometer, Model 14RI, equipped with a high-intensity source.

Solutions of the pyridine complexes were prepared by dissolving a weighed amount of the appropriate complex in a 10% pyridine solution of chloroform. This was necessary since these complexes readily lose two pyridine molecules.

The compounds were ground in Kel-F stopcock grease until a fine particle size was obtained. The resulting mull was then placed between two glass slides on the sample holder, then placed in a dewar filled with liquid nitrogen. A piece of filter paper saturated with Nujol was placed in the reference beam. Mulls were made up such that an absorbance of about 0.5 was obtained and the slits of the spectrophotometer were ≤ 0.7 mm in the near-infrared and ≤ 0.08 mm in the visible region. A beam attenuator

---

[12] G. Maki, *J. Chem. Phys.*, **28**, 651 (1958).

[13] C. R. Hare and C. J. Ballhausen, *ibid.*, **40**, 788 (1964). For completeness we give the matrix element $\langle ^3E_g(^3T_{2g})|V_{\mathrm{CF}}|^3E_g(^3T_{1g},{}^3F)\rangle = \sqrt{3}(Ds + {}^5/_4Dt)$.

[14] R. F. Fenske, D. S. Martin, Jr., and K. Ruedenberg, *Inorg. Chem.*, **1**, 441 (1962).

[15] C. J. Ballhausen, "Introduction to Ligand Field Theory," McGraw-Hill Book Co., Inc., New York, N. Y., 1962.

[16] Strictly speaking the $Ni(py)_4X_2$ is not D_{4h}, but C_{2v}; however, if we consider only the nitrogens of the pyridine ring and the anions, the system is D_{4h} and this symmetry will be assumed.

[17] See ref 15, Chapter 5.

[18] D. S. McClure, "Advances in the Chemistry of Coordination Compounds," S. Kirschner, Ed., The Macmillan Co., New York, N. Y., 1961, p 498.

was used when necessary to bring the pen onto the paper, and this was compensated for by increasing the light intensity of the high-intensity source.

Attempts to measure the polarized single-crystal spectra were unsuccessful. In all crystals that we looked at, dichroism was not observed either visually or spectrophotometrically when the crystal was rotated about a well-defined face. Consequently, nothing further was done with single-crystal polarized spectra.

Results and Discussion

$Ni(py)_4Br_2$.—In Table II we give the results of our mull and solution spectra, along with the calculated values and assignments.

Table II

Spectral Results for $Ni(py)_4Br_2$

ν, cm^{-1}			
10% py soln in chloroform	Mull spectra	Calcd	Assignment
8,000 (3.2)[a]	8,430 ± 15	8,420	$^3B_{1g} \rightarrow {}^3E_g$
11,200 (1.2)	11,490 ± 15	11,490	$\rightarrow {}^3B_{2g}$
12,400 (*b*)	12,260 ± 10	12,350	$\rightarrow {}^1A_{1g}({}^1D)$
	12,450 ± 10	12,360	$\rightarrow {}^1B_{1g}({}^1D)$
15,800 (4.4)	14,080 ± 10	14,090	$\rightarrow {}^3A_{2g}({}^3F)$
	16,390 ± 10	16,400	$\rightarrow {}^3E_g({}^3F)$
	...	19,540	$\rightarrow {}^1B_{2g}({}^1D)$
	21,040 ± 30	20,770	$\rightarrow {}^1A_{1g}({}^1G)$
		21,740	$\rightarrow {}^1E_g({}^1D)$
	...	24,950	$\rightarrow {}^3A_{2g}({}^3P)$
	...	25,680	$\rightarrow {}^1E_g({}^1G)$
25,400 (13.8)	26,030 ± 10	26,040	$\rightarrow {}^3E_g({}^3P)$

[a] The numbers in parentheses indicate ϵ in units of mole^{-1} cm^{-1} l. [b] Too weak to obtain an accurate value.

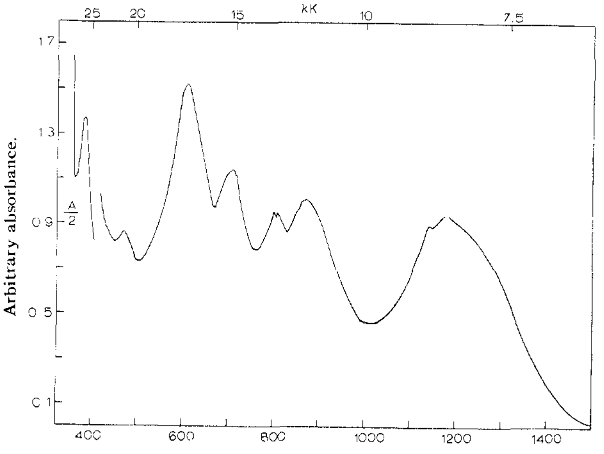

Figure 1.—Mull spectrum of $Ni(py)_4Br_2$ at liquid-nitrogen temperature.

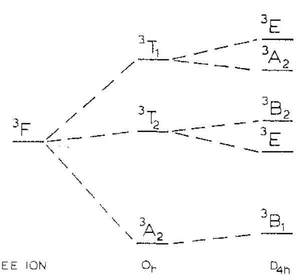

Figure 2.—Correlation diagram for the triplet states of a d^8 configuration. The subscript g has been left off for states in O_h and D_{4h} for clarity in presenting the diagram.

Before discussing the results, a discussion as to how the assignments of the spectra were made is appropriate here (see Figure 1). Considering the low-energy transitions first, the first two bands that occur are assigned to the transitions arising from the splitting of the $^3T_{2g}(F)$ in octahedral symmetry on going to D_{4h} symmetry (see Figure 2). The lowest energy transition is assigned to the ^3E_g transition and the next higher energy band to the $^3B_{2g}$ transition. The transition to the $^3B_{2g}$ state is dependent only on the in-plane field strength, $10Dq$ for pyridine, which is reported to be 10,000 cm^{-1} for $Ni(py)_6^{2+}$ in solution.[1] This transition is assigned to the band at 11,490 cm^{-1}. It is expected that the Dq value for pyridine would probably be greater in this complex than in $Ni(py)_6^{2+}$ because steric repulsions of the pyridines would be less in the tetragonal bromide complex. The fact that one complex is evaluated in solution and the other in the solid could also contribute to the difference. The transition to the ^3E_g state which is predominantly a function of $10Dq$ for pyridine and Dt then lies at 8430 cm^{-1}. The slight asymmetry of this transition can be attributed to a small deviation from D_{4h} symmetry or a dynamic Jahn–Teller effect.[19] As indicated by the spectrum of neat pyridine, the peak at ~8850 cm^{-1} is a pyridine overtone. These assignments are reasonable, since the crystal structure shows no anomalies in the Ni–Br distance or the Ni–N distance and pyridine is expected to have a greater Dq than Br^- resulting in a positive value for Dt[4] [$Dt = {}^4/_7(Dq^{xy} - Dq^z)$].

The next less intense doublet that is seen is composed of the components of ^1E_g arising in the octahedral field. It is interesting to note here that the two components of ^1E_g in D_{4h} symmetry are predicted to be degenerate. However, there is an off-diagonal coupling with the components of the other ^1E_g excited state. The off-diagonal coupling is not sufficient to explain the magnitude of the observed splitting, but since we have neglected spin–orbit coupling and this is the accepted mechanism by which spin-forbidden bands become allowed, this is not surprising.

The next two bands that are observed arise from the splitting of $^3T_{1g}(F)$ when the symmetry decreases from O_h to D_{4h}. In contrast to the components of the $^3T_{2g}$, the components of $^3T_{1g}({}^3F)$ depend to a first order on both Dt and Ds. Since we have determined the sign of Dt from our first assignment, there remains only to determine the magnitude and sign of Ds. We assigned both a positive and negative number to Ds and then attempted a quantitative fit of all the bands in the electronic spectrum. With a negative Ds, agreement between experiment and theory could not be obtained. Therefore calculations were performed with a positive Ds. This sign would be expected in a complex with axial

(19) F. A. Cotton and M. D. Meyers, *J. Am. Chem. Soc.*, **82**, 5023 (1960).

elongation.[20] The result of the computer calculations and assignments are given in Table II. In Table III we give the values of B, C, Dq, Ds, and Dt obtained.

TABLE III

SPECTRAL PARAMETERS FOR $Ni(py)_4X_2$ IN CM^{-1}

Parameter	$Ni(py)_4Br_2$	$Ni(py)_4Cl_2$
B	810 ± 1	820 ± 0.5
C	3130	3260
Dq	1150 ± 3	1173 ± 3
Dt	316 ± 0	283 ± 1
Ds	635 ± 3	480 ± 8
$\delta\pi$	−156	−10
$\delta\sigma$	−1540	−1240

For our calculations, the band maximum was assumed to be the $0 \rightarrow 0$ vibrational transition, although this may not be the case.[21] Since we have not observed any vibrational fine structure, this must be assumed. The error limits given in Table III result from the fact that, by taking different starting points, the calculated values of the parameters varied by this amount while giving transition energies which agreed with observed values within experimental error.

In addition, this assignment is supported by interpretation of the parameters in McClure's theory. By use of eq 2 and 3, $\delta\pi$ and $\delta\sigma$ are calculated to be −156 and −1540 cm^{-1}, respectively. Based on "chemical intuition," the σ bonding of pyridine should be greater than that of bromide ion and consequently the antibonding levels should be raised more in the former. As a result $\delta\sigma$ should be a large negative number ($\delta\sigma = \sigma_z - \sigma_{xy}$).

Therefore our assignments seem to be reasonable and are also supported by the excellent agreement obtained between calculations and experimental results.

The next peak is assigned to two spin-forbidden bands, ${}^1E_g\{{}^1T_{2g}({}^1D)\}$ and ${}^1A_{1g}\{{}^1A_{1g}({}^1G)\}$, and the last band is one component of the ${}^3T_{1g}$ in octahedral symmetry that arises from the ${}^3P$ free-ion term. It is assigned to the transition to the ${}^3E_g$ state. A detailed inspection of the spectra in this region does not indicate any shoulder that could be assigned to the ${}^3A_{2g}$ transition. However, since the band is positioned on the edge of the charge-transfer band and since the slits of the spectrophotometer were opening rapidly, it is not surprising that a shoulder could not be seen even if one is present. Alternatively, the intensity of the ${}^3A_{2g}$ transition may be small compared to that of ${}^3E_g$, and the ${}^3A_{2g}$ transition is effectively "washed out" by the intense charge-transfer transition and ${}^3E_g$ transition.[21a]

$Ni(py)_4Cl_2$.—The spectral results for $Ni(py)_4Cl_2$ are given in Table IV and Figure 3 along with the calculated results and assignments. The values of B, C, Dq, Dt, and Ds are given in Table III. The transitions were assigned in the same manner as the $Ni(py)_4Br_2$. The calculated energies and observed energies again are in good agreement with each other. The values of $\delta\pi$ and $\delta\sigma$ are −10 and −1240 cm^{-1} which seem to be consistent.

TABLE IV

SPECTRAL DATA FOR $Ni(py)_4Cl_2$

ν, cm^{-1}			
10% py in CH_3Cl	Mull spectra	Calcd	Assignment
8,650 (3.1)[a]	9,042 ± 20	9,036 ± 15	${}^3B_{1g} \rightarrow {}^3E_g({}^3F)$
10,250 (2.2)	11,730 ± 20	11,730 ± 20	$\rightarrow {}^3B_{2g}({}^3F)$
	12,620 ± 10		$\rightarrow {}^1A_{1g}({}^1D)$
12,500 (1.2)		12,700 ± 5	
	12,804 ± 10		$\rightarrow {}^1B_{1g}({}^1D)$
	14,930 ± 100	15,042 ± 20	$\rightarrow {}^3A_{2g}({}^3F)$
15,800 (5.1)			
	16,818 ± 15	16,831 ± 10	$\rightarrow {}^3E_g({}^3F)$
	...	20,867 ± 20	$\rightarrow {}^1B_{2g}({}^1D)$
		21,336 ± 10	$\rightarrow {}^1A_{1g}({}^1G)$
	21,768 ± 40		
		22,595 ± 10	$\rightarrow {}^1E_g({}^1D)$
	...	25,812 ± 15	$\rightarrow {}^3A_{2g}({}^3P)$
	...	26,239 ± 20	$\rightarrow {}^1E_g({}^1G)$
25,400 (10.7)	26,759 ± 40	26,727 ± 10	$\rightarrow {}^3E_g({}^3P)$

[a] The numbers in parentheses indicate ϵ in units of $mole^{-1}$ cm^{-1} l.

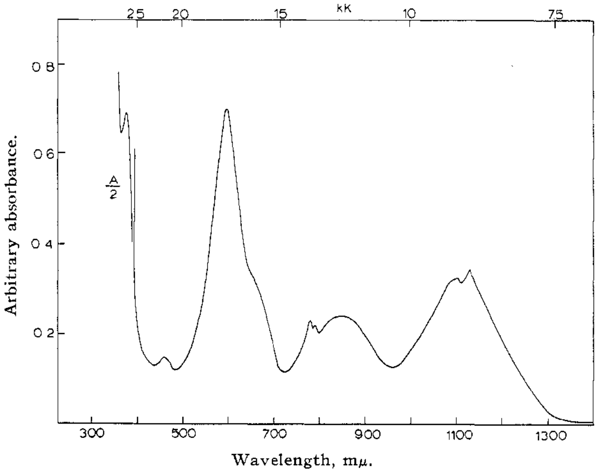

Figure 3.—Mull spectrum of $Ni(py)_4Cl_2$ at liquid-nitrogen temperature.

There are several literature reports indicating that Dq for Cl^- is greater than the Dq for Br^-. Since the ${}^3B_{2g}$ band indicates the Dq^{xy} for pyridine is essentially the same in both complexes, the $\delta\sigma$ for $Ni(py)_4Cl_2$ should be greater than the $\delta\sigma$ for $Ni(py)_4Br_2$ as is observed.

There is a small decrease in Dq^{xy} for pyridine on going from $Ni(py)_4Cl_2$ to $Ni(py)_4Br_2$. This is probably due to the lengthening of the Ni–N bond as is evidenced by the crystal structure.[11] This is in direct contrast to the solution data. In solution it appears that, as the Dq of the axial ligand decreases, the Dq of pyridine in the equatorial plane increases.

The available data are presented in Table V. The increase of the Dq of pyridine in the bromide complex can result from an increased charge on the metal ion resulting from a decrease in the covalent bonding ability of bromide relative to chloride.

This order of covalency for chloride and bromide is

---

[20] T. S. Piper and R. L. Carlin, *J. Chem. Phys.*, **33**, 1208 (1960).

[21] R. Dingle, *Acta Chem. Scand.*, **20**, 1435 (1966).

[21a] NOTE ADDED IN PROOF.—These assignments are the same as those reported [D. M. L. Goodgame, M. Goodgame, M. A. Hitchman, and M. J. Weeks, *J. Chem. Soc., Sect. A*, 1769 (1966)] in an article that appeared subsequent to the submission of ours. The spectral parameters were not properly evaluated and differ appreciably from those reported here.